Stick-Slip Operation of the Modular Distributed Manipulator System

Jonathan Luntz, William Messner, and Howie Choset
Department of Mechanical Engineering
Carnegie Mellon University

Abstract

The Modular Distributed Manipulator System (MDMS) is a novel materials handling system which is a fixed array of actuated wheels capable of inducing arbitrary motions in the plane. The wheels transport and manipulate objects that rest on the array. The motion of the object is determined by a combination of object weight distribution, actuator dynamics, speed control law, and friction between the wheels and the manipulated object. This work focuses on a stick-slip friction model and its impact on the dynamics of an object on the array. Factors such as coefficient of friction and object size and weight determine which wheels roll and which wheels slide relative to the object. This paper determines the ranges of parameters for which all wheels are in either sliding contact or rolling contact. Simulations are performed to demonstrate the dynamics of the system.

1 Introduction

The Modular Distributed Manipulator System (MDMS) both transfers and manipulates objects in the plane, enhancing applications such as flexible manufacturing and package handling systems. The MDMS combines the benefits of conveyor and robotic transport systems while overcoming their limitations by both transporting and manipulating large, heavy objects. This alternative method comprises a fixed array of actuators that cooperate to handle objects. The objects are significantly larger than each cell; several cells support an object that can be made to translate and rotate in the plane. Since sensing and actuation are distributed, each of many objects can be manipulated independently. (see Figure 1).

A prototype system was built consisting of a small array of cells capable of transporting objects about the size of a bread box. Each cell consists of a pair of orthogonally oriented motorized roller wheels (Figures 2 and 3) which are capable of producing a force perpendicular to their axes, while allowing free motion parallel to their axes. The combined action of these two wheels in to produce an arbitrary vectored motion in the plane. Currently, the prototype system consists of 18 cells which can be arranged either in a 1-D or a 2-D grid, shown in the photograph in Figure 4. Each cell is controlled by its own microcontroller, and motions are coordinated through communication between neighboring cells. For a more complete description of hardware and communication, see [6].

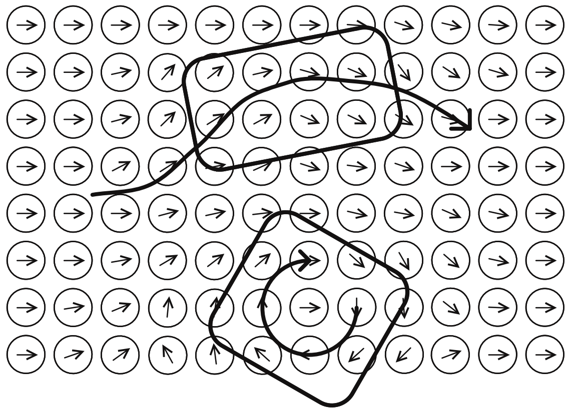

Figure 1: MDMS: Several objects can be translated and rotated, independently.

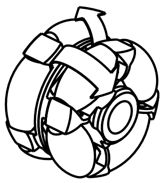

Figure 2: Roller wheel.

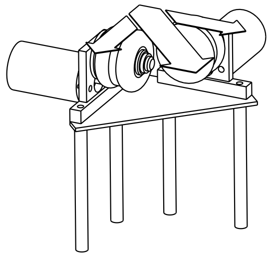

Figure 3: Prototype cell.

Towards the development of control laws and policies to provide desired object motions, this paper analyzes the dynamics of an object on a single row of cells moving in 1-D with both sliding and rolling friction contacts. In particular, limits on reference speed for rolling contact (stick) and sliding contact (slip) are derived under proportional control of motor speeds. This paper is organized as follows: Prior work leading to distributed manipulation is summarized in Section 2. The forces acting on an object are calculated in Section 3. Limits on reference speeds are presented in Section 4, along with simulations of the system.

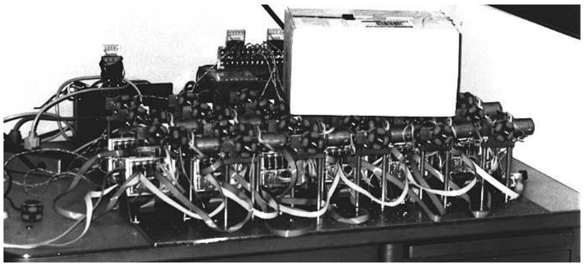

Figure 4: Current experimental setup.

2 Prior Work

Mason and Erdmann [1, 3] provided a radical alternative to standard robotic manipulation by significantly simplifying the robot manipulator and developing manipulation algorithms for these low-degree-of-freedom sensorless mechanisms. Goldberg [4] developed an algorithm which orients to symmetry a part with a sequence of gripper open, close, and rotation operations without sensor information. This sequence of operations is termed a *squeeze*.

Böhringer, Donald, et. al. [2] applied this type of sensorless manipulation to an array of micromechanical actuators which was used to manipulate very small objects with the application of "squeeze fields". Kavraki [5] supplied further analysis of microactuated systems using elliptical potential fields to orient an object to symmetry without sensors. These microactuated systems differ from the authors work in that on such a small scale, mass, friction, and array resolution may be ignored.

In previous papers by the authors [7, 8, 9] motions of objects on the MDMS both in 1-D and in 2-D with rotation were analyzed, and a velocity field was designed which can position and orient certain symmetric objects within cell resolution and symmetry. This analysis assumed full sliding friction between the wheels and the object without considering motor dynamics. In reality, both sliding and rolling contact is made with the object, and in a rolling mode, the motor's dynamics come into play. This paper takes a first step towards controlling object's motions using both stick and slip friction by analyzing the motion of objects in both friction modes in 1-D on a single row of cells.

3 Analysis of Forces on an Object

To analyze the dynamics of an object the horizontal forces on the object must be determined. The total horizontal force is the sum of the forces applied by the wheels in rolling contact with the object and the forces applied by the wheels in sliding contact with the object. To determine which wheels are sliding and which are rolling, it is necessary to determine the normal forces supporting the object. Using vertical and rotational equilibrium

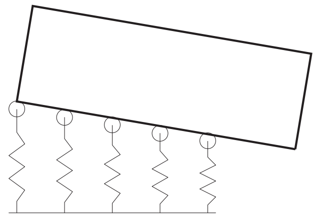

Figure 5: Flexible cells support a flat object.

along with the assumptions that each cell provides a linear spring support and that the bottom of the object is flat (as shown in Figure 5), it was shown in [9] that the collection of normal forces exerted by each contact written as a vector $\vec{N} = [N_1 \ \ldots \ N_n]^{\mathrm{T}}$ is equal to

$$\vec{N}^{\mathrm{T}} = \mathbf{B}^{\mathrm{T}} \left(\mathbf{B}\mathbf{B}^{\mathrm{T}}\right)^{-1} \begin{bmatrix} W \\ W x_c \end{bmatrix} \tag{1}$$

where W is the weight of the object, x_c is the location of the object's center of mass, and $\mathbf{B} = \begin{bmatrix} 1 & \ldots & 1 \\ x_1 & \ldots & x_n \end{bmatrix}$ with x_i being the position of the i^{th} cell supporting the object. The matrix $\mathbf{B}$ will change as the object moves changing the set of supporting cells, but is constant while the object remains on a single set of supports.

To determine when all wheels are in rolling contact and when all wheels are in sliding contact, the maximum and minimum normal forces supporting an object must be known. Equation 1 shows that the normal forces over all the supporting cells vary linearly with cell position x_i. Thus the maximum and minimum supporting forces will be applied by the cells at the ends of the object.

Equation 1 also shows that the supporting force at each cell varies linearly with the position of the object, x_c. Therefore, there can be no local extrema in normal force with respect to cell position, and the minimum and maximum supporting forces will occur at discontinuities, i.e. just before or just after the set of supporting cells change. For uniform cell spacing d and an object of length $L > 2d$, there exists an integer $m \geq 2$ and a non-negative real number $h < 1$ such that $L = d\,(m+h)$. An object will rest on either m or $m+1$ cells. Assuming that the center of mass of the object is at its geometric center, by examining the four extreme cases, the minimum and maximum normal forces over all positions of an object can be expressed as

$$\begin{aligned} N_{min} = \min \Bigg(& \frac{1}{m+1} - \frac{3}{(m+1)\,(m+2)} h \,, \\ & \frac{m-2}{m\,(m+1)} + \frac{3}{m\,(m+1)} h \Bigg) W \end{aligned} \tag{2}$$

$$\begin{aligned} N_{max} = \max \Bigg(& \frac{1}{m+1} + \frac{3}{(m+1)\,(m+2)} h \,, \\ & \frac{m+4}{m\,(m+1)} - \frac{3}{m\,(m+1)} h \Bigg) W \end{aligned} \tag{3}$$

3.1 Sliding Contact

The case where the wheels always slip on the object was studied in previous papers by the authors in the 1-D and 2-D cases with both coulomb and viscous friction laws [7, 8, 9]. A summary of the 1-D case under coulomb friction is presented here.

When sliding friction exists between the wheels and the object, each cell is assumed to apply a horizontal force proportional to the normal force and to the coefficient of friction in the direction of motion of the wheel. For full-slip friction, it is required that the wheels spin much faster than the object moves. (This condition is discussed in more detail in a following section.) Assuming this is the case over the entire array, each wheel applies a horizontal force $f_i = \mu \mathrm{sign}\left(v_i\right) N_i$. These forces can be added through the use of the inner product to provide a net force on the object.

$$f = \sum f_i = \mu \mathrm{sign}\left(\left[v_1 \, \dots \, v_n\right]\right) \vec{N}^{\mathrm{T}} \tag{4}$$

Taking the normal force vector $\vec{N}$ from Equation 1,

$$f = \mu W \mathrm{sign}\left(\left[v_1 \, \dots \, v_n\right]\right) \mathbf{B}^{\mathrm{T}} \left(\mathbf{B}\mathbf{B}^{\mathrm{T}}\right)^{-1} \begin{bmatrix} 1 \\ x_c \end{bmatrix} \tag{5}$$

The constant and x_c terms can be separated, and terms grouped to yield mass-spring type dynamics

$$f = k_s^s x_c + f_o^s \tag{6}$$

The spring constant k_s^s and the offset force f_o^s are defined in terms of the velocities and positions of cells supporting the object, as well as coefficient of friction μ and the object's weight W. k_s^s and f_o^s are constant while the object is on a particular set of supports, an change values when the object changes supports.

3.2 Rolling Contact

When the wheels roll without slipping on the object, the velocities of the wheels v_i are equal to the velocity of the object $\dot{x}_c$. It is therefore necessary to include actuator dynamics and the motor speed control law when determining the total forces acting on the object.

The wheels in the MDMS prototype are driven by simple DC motors through a single gear reduction. The relation between linear speed of the i^{th} wheel's outer radius v_i, tangential force developed by the wheel f_i, and voltage applied to the motor V_i is

$$f_i \frac{r_w}{N_g} = \left(V_i - v_i \frac{N_g}{r_w} K_m\right) \frac{K_m}{R_m} - v_i \frac{N_g}{r_w} B_m \tag{7}$$

where R_m, B_m, and K_m are the motor's coil resistance, damping, and torque constant, r_w is the wheel's radius, and N_g is the gear ratio between the motor and wheel. These constants can be lumped into an effective motor constant $K_e = K_m \frac{N_g}{r_w}$ and an effective damping $B_e = B_m \frac{{N_g}^2}{{r_w}^2}$. These effective constants relate linear motions and forces at the wheel's outer radius to motor voltage.

$$f_i = V_i \frac{K_e}{R_m} - v_i \left(B_e + \frac{{K_e}^2}{R_m}\right) \tag{8}$$

Under closed-loop proportional control, with gain G and reference speed r_i such that $V_i = G\left(r_i - v_i\right)$ the motor speed-force relationship becomes

$$f_i = r_i \frac{K_e G}{R_m} - v_i \left(B_e + \frac{{K_e}^2}{R_m} + \frac{G K_e}{R_m}\right) \tag{9}$$

The force each cell applies to the object is then a function of the motor dynamics from Equation 8 with $\dot{x}_c$ substituted for each v_i. For n cells supporting the object, these forces can be summed to produce a net horizontal force on the object. Assuming that each motor is identical, with only r_i differing between cells, the force on the object becomes

$$f = \frac{K_e G}{R_m} \sum r_i - \dot{x}_c n \left(B_e + \frac{{K_e}^2}{R_m} + \frac{G K_e}{R_m}\right) \tag{10}$$

which can be rewritten as

$$f = f_o^r - \dot{x}_c b^r \tag{11}$$

The constant force f_o^r is proportional to the sum of the cells' reference velocities under the object. The object will be in equilibrium when $\sum r_i = 0$.

4 Parameter Ranges

In general, it is possible for some cells to be in a sliding contact mode and others to be in a rolling contact mode. Since it is difficult to predict motions of an object with mixed contact modes, it is generally desired that all the wheels under the object be in one of the two contact modes depending on the application. For example, full sliding contact can be used when implementing an open-loop (passive) policy to accurately position an object by taking advantage of the mass-spring dynamics. For a closed-loop (active) policy, full rolling contact is often desired to maintain better control over the motion of the object since the motion of the object can be measured directly from the rotations of the wheels.

4.1 Full Rolling Conditions

If the horizontal force due to from rolling friction at a wheel becomes greater than the force from sliding friction, then that wheel breaks free into sliding contact. This assumes that the coefficient of static friction is equal to the coefficient of sliding friction. This assumption applies in the existing hardware because the

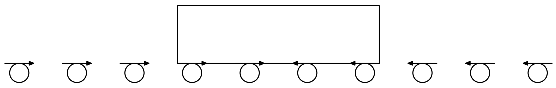

Figure 6: Inward pointing field positions an object.

"bumpy" roller wheels provide ample opportunity to break static friction effectively eliminating hysteresis. In terms of motor parameters, rolling friction occurs when

$$\mu N_i > \left| r_i \frac{K_e G}{R_m} - \dot{x}_c \left(B_e + \frac{{K_e}^2}{R_m} + \frac{GK_e}{R_m} \right) \right| \qquad (12)$$

To guarantee full-stick friction for all the cells for all motions of the object, the extreme case must be considered, that is where N_i is at its smallest possible value, r_i is at its largest positive value, and $\dot{x}_c$ is at its largest negative value (or equivalently, negative r_i and positive $\dot{x}_c$). Equation 12 can be enforced for all cells by selecting $r_i = \max |r_i|$ and $\dot{x}_c = -\max |r_i|$ (because the object never can go faster than the fastest wheel). N_{min} is determined for the current object from Equation 2.

$$\begin{aligned} \mu N_{min} &> \max |r_i| \frac{K_e G}{R_m} + \\ &\quad \max |r_i| \left(B_e + \frac{{K_e}^2}{R_m} + \frac{GK_e}{R_m} \right) \\ \mu N_{min} &> \max |r_i| \left(B_e + \frac{{K_e}^2}{R_m} + 2\frac{GK_e}{R_m} \right) \qquad (13) \end{aligned}$$

Equation 13 can be used to compute a maximum allowable reference speed providing a conservative bound on wheel reference speed.

$$r_i^{max} = \frac{\mu N_{min}}{B_e + \frac{{K_e}^2}{R_m} + 2\frac{GK_e}{R_m}} \qquad (14)$$

It is not possible, in general, to guarantee full sliding contact for all motions of an object. For example, if all wheels rotate in the same direction, the speed of the object will eventually reach that of the wheels, and stick friction will occur. What is more relevant is that the object will experience full sliding contact at equilibrium.

4.2 Equilibrium Conditions

A common application for a single row of cells is to position an object with an inward-pointing velocity field where all cells to the right of the origin rotate to the left, and all cells to the left of the origin rotate to the right as shown in Figure 6. In this case, all cells have the same magnitude reference speed.

Near the equilibrium position, the behavior of the object can be predicted depending on the contact mode. With full rolling contact, the object may come to rest in any position, as long as equal numbers of cells are covered on either side. With full sliding contact, the net horizontal force on the object is a linear function of the object's position, and equilibrium occurs only when the object's center of mass is at the origin.

For a passive policy to accurately position an object, full sliding friction must occur at equilibrium. To ensure this, rolling friction forces for all cells must be larger than coulomb friction forces so that sliding friction occurs. This condition must be true when the object is centered such that the weight of the object is distributed equally among the supports. The extreme case, must be examined, so $r_i = \min |r_i|$. To maintain full sliding contact, the following relation must hold.

$$\mu \frac{W}{k+1} < \min |r_i| \frac{GK_e}{R_m} \qquad (15)$$

where $k = m$ for m odd, and $k = m - 1$ for m even. This provides a minimum allowable reference speed.

$$r_i^{min} = \frac{\mu \frac{W}{k+1}}{\frac{GK_e}{R_m}} \qquad (16)$$

To maintain full stick friction at equilibrium, a similar restriction is obtained which provides a maximum reference speed. Selecting the minimum possible normal force N_{min} provides the extreme case (since rolling equilibrium does not necessarily occur at $x_c = 0$). Thus, r_i must be less than

$$r_i^{max} = \frac{\mu N_{min}}{\frac{GK_e}{R_m}} \qquad (17)$$

4.3 Simulations

A Simulink model was created to simulate the motion of an object on the field described in Section 4.2. In the simulations, motor constants and other parameters were chosen to be representative of (but not necessarily equivalent to) the actual system. The following values were used: $r_w = 1in$, $N_g = 3$, $K_m = .024Nm/A$, $R_m = 5\Omega$, and $B_m = 3.5 \times 10^{(} - 6)Nms$. 10 cells are spaced at $5in$ intervals with the origin halfway between cells. A gain of $G = 10Vs/m$ was used. A $2kg$ object with a length of 3.5 cell spacings starts near the left end of the row. The coefficient of friction was selected to be $\mu = 0.3$. The motor reference speeds were held constant.

Three values of r were used to represent the different contact modes. Figure 7 shows a full rolling contact case where $r = r_i^{max} = 0.0635m/s$ from Equation 14. Here, the object slowly reaches equilibrium just after it touches the second cell after the origin. Figure 8 shows a full sliding contact case using a fast $r = 10m/s$. Here, the object simply oscillates with constant magnitude. In reality, however, some damping exists, and the object will reach equilibrium at the origin. Figure 9 shows a mixed contact case using $r = 0.75m/s$ which is well above the minimum for full sliding equilibrium of

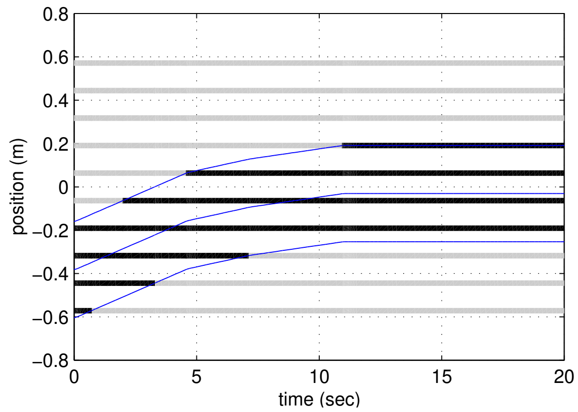

Figure 7: Simulation of full rolling contact. In this and the two following figures, object position is plotted over time. The three traces represent the positions of the two ends and the middle of the object. The horizontal bands represent cell position, with color representing contact type (light grey = no contact, medium grey = sliding contact, black = rolling contact).

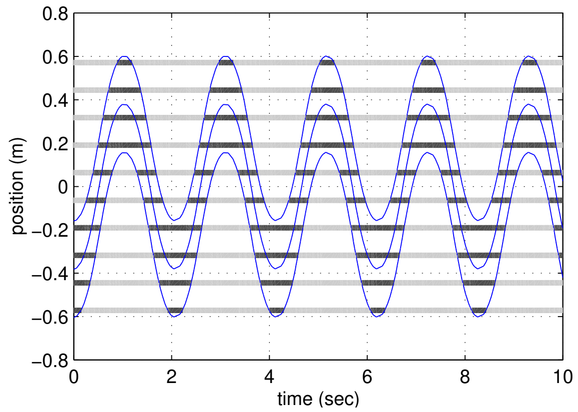

Figure 8: Simulation of full sliding contact.

$r_i^{min} = 0.21 m/s$ from Equation 16. The object starts oscillating with a large magnitude with some wheels sticking, providing damping, and settles into a steady state oscillation as fewer wheels stick.

5 Conclusions and Future Work

Stick-slip friction modeling was performed for the MDMS using the distribution of weight of an object on a regularly spaced 1-D array, coulomb friction, a simple DC motor model, and proportional speed control. Limits on the reference wheel speeds for all wheels to be in either rolling or sliding contact with an object were determined. Simulink based simulations verified the analytical predictions.

Future work will address two-dimensional stick slip modeling including object rotation, along with extensions to viscous friction sliding interface.

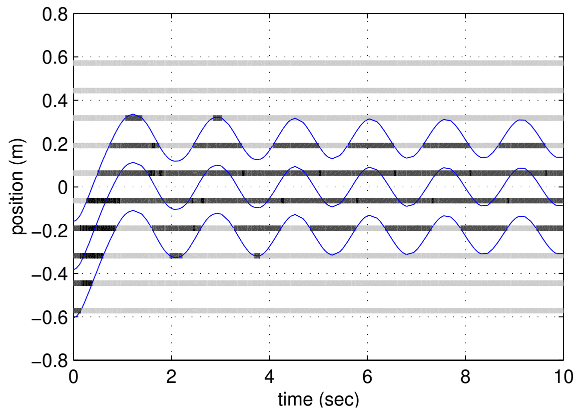

Figure 9: Simulation of mixed contact.

References

[1] S. Akella, W. Huang, K. Lynch, and M. Mason. Sensorless parts feeding with a one joint robot. In *Proceedings. Workshop on the Algorithmic Foundations of Robotics*, 1996.

[2] K. Böhringer, B. Donald, R. Mihailovich, and N. MacDonald. A theory of manipulation and control for microfabricated actuator arrays. In *Proceedings. IEEE International Conference on Robotics and Automation*, 1994.

[3] M. Erdmann. An exploration of nonprehensile two-palm manipulation: Planning and execution. In *Proceedings. Seventh International Symposium on Robotics Research*, 1995.

[4] K. Goldberg. Orienting polygonal parts without sensors. *Algorithmica: Special Issue on Computational Robotics*, 10:201–225, August 1993.

[5] L. Kavraki. Part orientation with programmable vector fields: Two stable equilibria for most parts. In *Proceedings. IEEE International Conference on Robotics and Automation*, 1997.

[6] J. Luntz and W. Messner. A distributed control system for flexible materials handling. *IEEE Control Systems Magazine*, 17(1), February 1997.

[7] J. Luntz, W. Messner, and H. Choset. Parcel manipulation and dynamics with a distributed actuator array: The virtual vehicle. In *Proceedings. IEEE International Conference on Robotics and Automation*, 1997.

[8] J. Luntz, W. Messner, and H. Choset. Virtual vehicle: parcel manipulation and dynamics with a distributed actuator array. In *Proceedings of SPIE vol. 3201. Sensors and Controls for Advanced Manufacturing. International Symposium on Intelligent Systems and Advanced Maufacturing.*, 1997.

[9] J. Luntz, W. Messner, and H. Choset. Velocity Field Design on the Modular Distributed Manipulator System. In *Proceedings. Workshop on the Algorithmic Foundations of Robotics.*, 1998.